ACS Partner Journal

CHEM & BIO ENGINEERING

pubs.acs.org/ChemBioEng

Article

NH_2-MIL-125 Nanosheets Prepared via Crystallization Kinetics Modulation for Ultrathin Membrane Fabrication

Published as part of Chem & Bio Engineering virtual special issue "Framework Materials".

Yanwei Sun, Jiahui Yan, Mingming Wu, Jie Jiang, and Yi Liu*

Cite This: *Chem Bio Eng.* 2024, 1, 855−862

Read Online

ACCESS | Metrics & More | Article Recommendations | Supporting Information

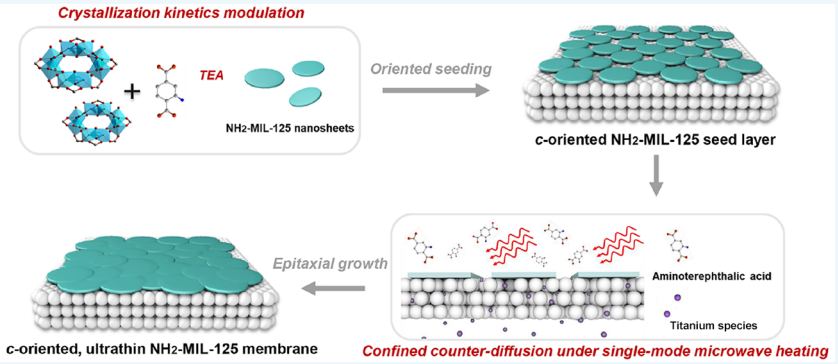

ABSTRACT: Regulating both crystallographic orientation and thickness of titanium metal−organic framework (Ti-MOF) membranes remains a significant challenge. In this study, we pioneered the fabrication of uniform 29 nm thick NH_2-MIL-125 nanosheet seeds by employing crystallization kinetics modulation approach. Through innovating confined counter-diffusion-assisted epitaxial growth under single-mode microwave heating, a highly *c*-oriented 80 nm thick NH_2-MIL-125 membrane was prepared. Significant reduction in thickness endowed the membrane with unprecedented H_2 permeance (1350 GPU) along with considerable H_2/CO_2 selectivity (19.1), exceeding the performance benchmarks of state-of-the-art NH_2-MIL-125 membranes.

KEYWORDS: *MOF, nanosheets, gas separation, orientation, ultrathin membrane*

1. INTRODUCTION

Metal−organic frameworks (MOFs) constitute crystalline materials featured with high porosity, tailorable pore size, and rich functionality, making them appealing for widespread applications such as catalysis, gas storage, and separation.[1−6] Among them, titanium-based MOFs (Ti-MOFs) have garnered significant attention due to their high thermal stability. As a prototypical member of Ti-MOFs, NH_2-MIL-125, which is synthesized from TPOT and 2-aminoterephthalic acid (NH_2-BDC), represents a promising candidate for membrane-based CO_2 separation based on its suitable pore size, strong CO_2 affinity, and remarkable chemical robustness.[7−9] Our recent findings highlighted that maintaining preferred *c*-orientation was beneficial for enhancing H_2/CO_2 separation performance of NH_2-MIL-125 membranes.[10,11] To overcome the trade-off limitation between permeance and selectivity, achieving a significant reduction in membrane thickness has become indispensable. Recently, by using TiS_3 as titanium source during epitaxial growth, we successfully prepared 380 nm thick NH_2-MIL-125 membrane.[11] Nonetheless, further reducing its thickness to the sub-100 nm level has encountered significant challenges, owing to the difficulties in minimizing thickness of seed layer and preventing excessive epitaxial growth.

Epitaxial growth of MOF nanosheets (NSs) has been considered as a reliable strategy for the preparation of oriented MOF membranes with ultrathin thickness.[12−14] Recent decades have witnessed notable progress in the synthesis of MOF NSs. However, the majority of methods developed so far have primarily focused on 2D MOF materials with layered frameworks. In contrast, only a few approaches aiming at the synthesis of MOF NSs with a 3D topology have been documented. For instance, Seoane prepared NH_2-MIL-53(Al) NSs with thicknesses in the range of 35−45 nm by utilizing a surfactant-assisted approach.[15] This method involved the use of cationic surfactant hexadecyltrimethylammonium bromide

Received: May 13, 2024
Revised: July 11, 2024
Accepted: July 16, 2024
Published: July 29, 2024

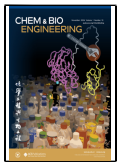

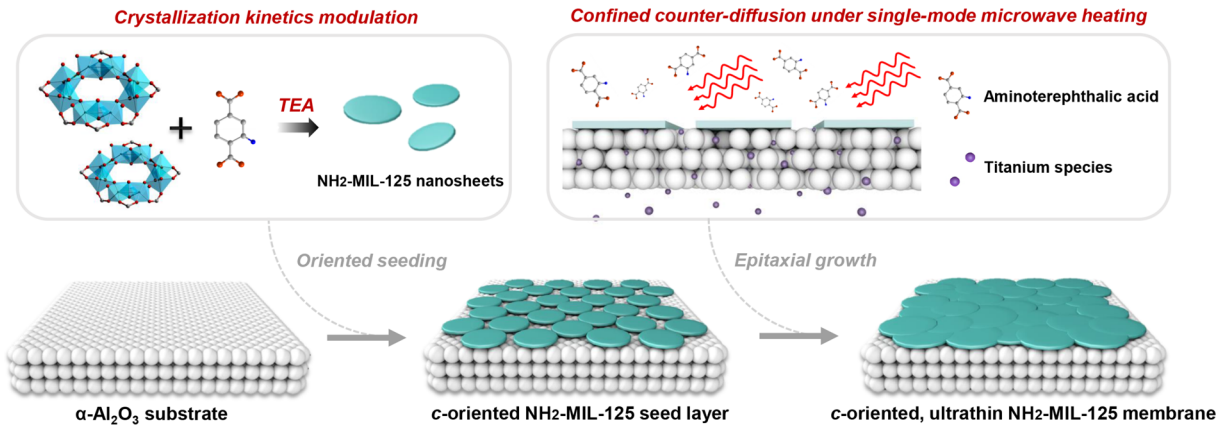

Figure 1. Scheme illustration of the preparation of highly *c*-oriented ultrathin NH_2-MIL-125 membrane.

as a growth modulator. Recently, Zhu achieved a breakthrough through preparing 2.7 nm thick MOF-74 NSs via a surfactant-free method. 1.2 nm thick iron−cobalt oxide NSs served as the sacrificial template.[16] However, the exploration of Ti-MOF NSs remains in its infancy, largely hindered by strong metal−ligand bonds. Therefore, developing innovative approaches for producing uniform MOF NSs has become indispensable.

Exerting precise control over crystallization kinetic has been proven to be effective for regulating MOF structure and morphology.[17−19] The key to precise control over crystallization kinetics includes the type of precursor source and the reaction medium. For instance, Gascon conducted an in-depth study on kinetic control of NH_2-MIL-101(Al) and NH_2-MIL-53(Al) crystallization through time-resolved in situ X-ray scattering;[20] moreover, 2D Cu-BDC NSs with adjustable thickness were further synthesized, capitalizing on the diffusion-mediated modulation of MOF growth kinetics.[21] Zhang revealed that proper environment of the reaction medium played a crucial role in governing the deprotonation rate of organic linkers, significantly influencing the size and morphology of Dy(BTC)(H_2O) crystals.[22] A series of advances have been made in morphology control of NH_2-MIL-125 crystals.[23−25] For instance, the morphology change from circular plates to octahedrons was realized through simple modulation of the concentration of reactants during crystallization.[26] Nevertheless, exerting precise control over the crystallization kinetics of NH_2-MIL-125 NSs remains to be explored.

Epitaxial growth has been demonstrated to enable accurate control over the microstructure of MOF membranes through decoupling nucleation and growth stages. Being analogous to MOFs, in the past decades, significant progress was made in epitaxial growth of *b*-oriented MFI zeolite membranes either.[27−30] However, several obstacles remain to be conquered. On the one hand, it is critical to avoid excessive growth without affecting membrane continuity; on the other hand, effective suppression of undesired twin growth during epitaxial growth remains indispensable. Therefore, it is imperative to prepare sub-100 nm thick and *c*-oriented NH_2-MIL-125 membranes through innovating the current synthetic protocol.

Motivated by the above concerns, in this study, we developed a crystallization kinetic modulation approach for the facile synthesis of highly uniform NH_2-MIL-125 NSs. During this process, triethylamine (TEA), serving as a nucleation modulator of NH_2-MIL-125 NSs, was added to the precursor solution. Subsequently, oriented deposition was conducted to prepare the NH_2-MIL-125 seed monolayer. Finally, sub-100 nm thick and highly *c*-oriented NH_2-MIL-125 membrane was obtained via confined counter-diffusion under single-mode microwave heating (Figure 1). Gas permeation results indicated that the H_2 permeance of the obtained NH_2-MIL-125 membrane outperformed state-of-the-art pure NH_2-MIL-125 membranes tested under similar conditions.

2. MATERIALS AND METHODS

2.1. Reagents and Materials. Titanium isopropoxide (TPOT, 99.9%, Aladdin), 2-aminoterephthalic acid (NH_2-BDC, 99.5%, Sigma-Aldrich), triethylamine (TEA, 99%, Aladdin), *N*,*N*-dimethylformamide (DMF, 99.8%, Tianjin Kermel), methanol (MeOH, 99.7%, Tianjin Kermel), and *n*-hexylamine (99%, Aladdin) were directly used without any additional purification. Porous α-Al_2O_3 ceramic discs with a diameter of 18 mm, thickness of 1 mm, and pore size of 70 nm were purchased from Fraunhofer IKTS (Germany). High-purity gases (H_2, CH_4, CO_2, N_2, and He) with a purity of 99.999% were supplied by Dalian Junfeng Gas Chemical Co., Ltd.

2.2. Synthesis of NH_2-MIL-125(*n*) Using TEA as Modulator. A 0.42 g portion of NH_2-BDC and a given amount of TEA were first dissolved in a mixture of 27 mL of DMF and 3 mL of MeOH under continuous stirring. Subsequently, 0.45 mL of TPOT was added to the above solution. The obtained mixture was then transferred into a 50 mL Teflon-lined autoclave. The autoclave was subjected to solvothermal treatment at 150 °C under static conditions for 24 h. Upon completion of the reaction, the autoclave was allowed to cool to room temperature. The solid product was subsequently isolated by centrifugation, followed by thorough washing with DMF and MeOH to remove any unreacted materials and byproducts. Finally, the product was dried in an oven at 60 °C overnight to yield NH_2-MIL-125(*n*) powders, where *n* refers to the molar concentration of added TEA.

2.3. Deposition of Seed Layer. To prepare the NH_2-MIL-125 seed suspension, 0.04 g of NH_2-MIL-125(0.56) was mixed with 5 mL of ethanol and stirred in a cone-shaped bottle at room temperature for an extended period of 6 days. Prior to oriented deposition, a precleaned porous α-Al_2O_3 plate was placed on a horizontal plane to ensure even coverage. The next step involved the careful positioning of a needle tip at the air/water interface. An automatic injector was then utilized to disperse the seed solution onto the water surface at controlled rate of 2 μL/min, aiming to form a continuous layer at the air−water interface. As the liquid layer gradually evaporated under controlled conditions, NH_2-MIL-125 seeds underwent self-assembly into a highly *c*-oriented monolayer on the substrate.

2.4. Epitaxial Growth of NH_2-MIL-125 Membrane. *2.4.1. Epitaxial Growth of NH_2-MIL-125 Membrane with Different Metal Sources under Single-Mode Microwave Heating.* 0.28 g of NH_2-BDC and 0.007 g of TiS_2 were dissolved in a solution containing 15

https://doi.org/10.1021/cbe.4c00103
Chem Bio Eng. 2024, 1, 855−862

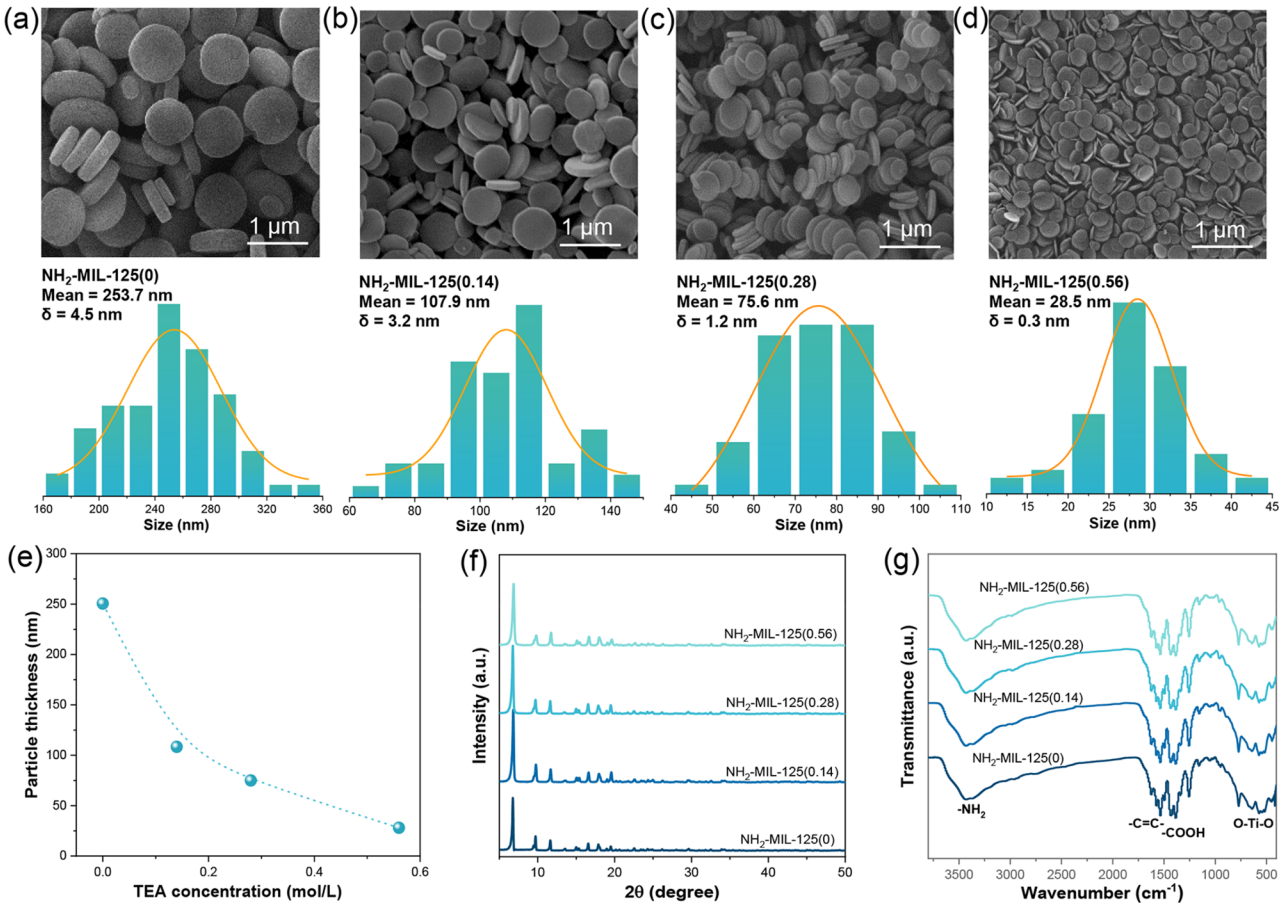

Figure 2. SEM images and particle size distributions of NH_2-MIL-125 powders prepared at 150 °C for 24 h with TEA concentrations of (a) 0, (b) 0.14, (c) 0.28, and (d) 0.56 mol L^{-1}. (e) Relationship between particle size and TEA concentration. (f) XRD patterns and (g) FTIR spectra of different NH_2-MIL-125 powders.

mL of DMF and 15 mL of MeOH with stirring. This clear solution was then transferred into an 80 mL vessel in which the seeded substrate was positioned vertically to facilitate uniform growth. Afterward, the vessel was sealed and placed in a single-mode microwave oven (Discover, CEM). The temperature rapidly escalated to 150 °C within 10 min and subsequently maintained at this temperature for 20 min. The system was allowed to cool down to ambient temperature. Resultant membrane was washed with copious of MeOH to remove any unreacted substances or byproducts. Finally, the membrane underwent drying at room temperature throughout the night to ensure thorough solvent evaporation.

For comparison, an identical protocol was utilized for preparation of the NH_2-MIL-125 membrane except that 0.02 mL of TPOT instead of 0.007 g of TiS_2 was employed as the metal source during epitaxial growth.

2.4.2. Epitaxial Growth of NH_2-MIL-125 Membrane Based on Confined Counter-Diffusion. Initially, 0.08 g of TiS_2 was ground with a mortar after addition of 0.1 mL of *n*-hexylamine. Subsequently, products were dispersed in a solution containing 1 mL of DMF and 1 mL of MeOH under sonication and then deposited on the back side of the seeded substrate. In the next step, the substrate was fixed in a homemade module and placed vertically in an 80 mL vessel filled with a mixture solution containing 0.28 g of NH_2-BDC, 15 mL of DMF, and 15 mL of MeOH. Afterward, the vessel was sealed and placed in a single-mode microwave oven (Discover, CEM). The temperature rapidly escalated to 150 °C within 10 min and subsequently maintained at this level for 20 min. Finally, the membrane was washed with MeOH and underwent drying at room temperature throughout the night to ensure thorough solvent evaporation.

2.5. Characterization. Powder X-ray diffraction (XRD) patterns were obtained using a Rigaku SmartLab diffractometer, employing Cu Kα radiation (λ = 0.15418 nm) with focused monochromated Cu Kα radiation at 45 kV and 200 mA. SEM images were captured by using a field emission scanning electron microscope (Hitachi FLEXSEM 1000). FT-IR spectra were recorded by utilizing a Nicolet iN10 infrared microscope (Thermo Fisher, USA).

2.6. Gas Permeation Test. Single gas permeation measurements were made for pure gases (H_2, CO_2, N_2, and CH_4). A constant feed flow of 50 mL min^{-1} was maintained for each gas being tested. Helium (He) with a flow of 50 mL min^{-1} was used as a sweep gas to facilitate the removal of gas from the permeate side. The pressure on both feed and permeate sides was held at 1 bar. The experimental temperature was held at 25 °C. The concentration of each gas on the permeate side was determined by gas chromatography (Agilent 7890B). The permeance is calculated using the equation

$$P_i = \frac{N_i}{\Delta P_i \times A}$$

In this equation, N_i (mol s^{-1}) corresponds to the molar flow rate of component *i*, ΔP_i (Pa) represents the transmembrane pressure difference for gas component *i*, and *A* (m^2) denotes the effective area of the membrane used in the experiment. The ideal selectivity $S_{i/j}$ for a pair of components *i* and *j* is computed based on the permeances of the two components according to the equation

$$S_{i/j} = \frac{P_i}{P_j}$$

Mixed gas permeation measurements were made at 25 °C for a mixture of H_2/CO_2 containing 50 mol % H_2. The feed flow rate remained constant at a volumetric rate of 50 mL min^{-1} for each gas. In all instances, helium was employed as the sweep gas, flowing at a

https://doi.org/10.1021/cbe.4c00103
Chem Bio Eng. 2024, 1, 855−862

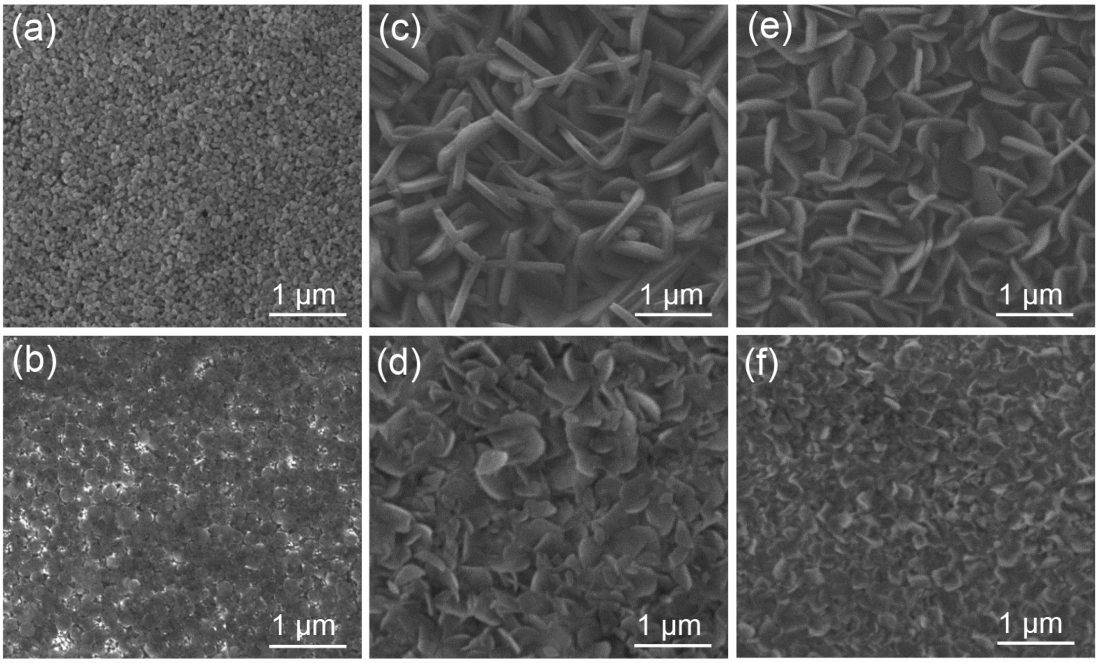

Figure 3. SEM images of (a) porous α-Al_2O_3 substrate, (b) NH_2-MIL-125 seed monolayer, and NH_2-MIL-125 membranes prepared under single-mode microwave heating with TiS_2 contents of (c) 1, (d) 0.5, (e) 0.25, and (f) 0.1 equiv.

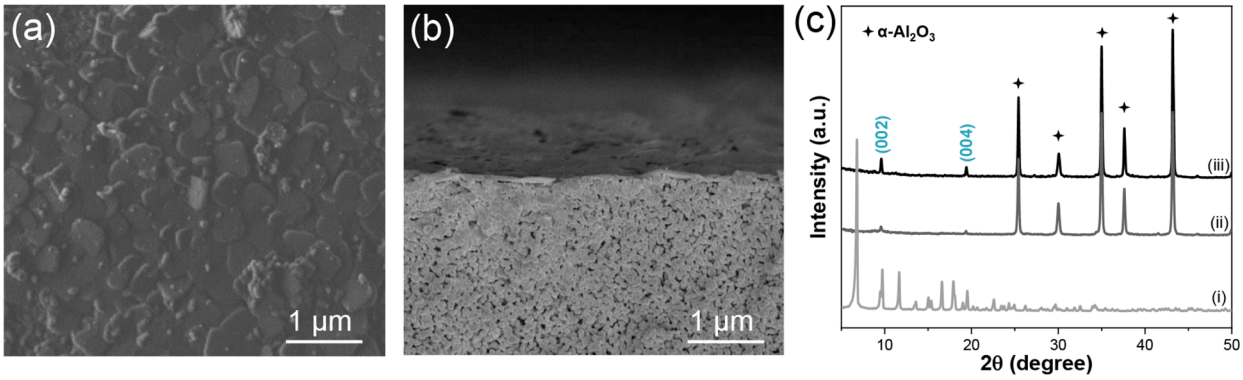

Figure 4. (a) Top and (b) cross-sectional SEM views of NH_2-MIL-125 membrane prepared by confined counterdiffusion under single-mode microwave heating. (c) XRD patterns of (i) NH_2-MIL-125 powders, (ii) NH_2-MIL-125 seed layer, and (iii) NH_2-MIL-125 membrane.

volumetric rate of 50 mL min^{-1}. The pressure on both feed and permeate sides was held at 1 bar. The separation factor, denoted as $\alpha_{i/j}$, is defined as the ratio of the molar proportions of components (i, j) on the permeate side divided by the ratio of the molar proportions of components (i, j) on the feed side:

$$\alpha_{i/j} = \frac{X_{i,\text{perm}}/X_{j,\text{perm}}}{X_{i,\text{feed}}/X_{j,\text{feed}}}$$

3. RESULTS AND DISCUSSION

3.1. Synthesis of NH_2-MIL-125 NS Seeds. The role of TEA as a nucleation modulator in the formation of NH_2-MIL-125 NSs is vividly depicted in SEM images. In the absence of TEA, NH_2-MIL-125 displayed a disk-shaped morphology with an average thickness of 253.7 ± 4.5 nm (Figure 2a). It has been proved that the crystallization of carboxylate-based MOFs was largely determined by the degree of deprotonation of carboxylic linkers. In the absence of TEA, NH_2-BDC showed a low degree of deprotonation, relying on the decomposition of DMF at high temperatures to produce dimethylamine. This condition typically resulted in a slow nucleation process followed by their rapid growth, leading to the formation of large NH_2-MIL-125 crystals. Conversely, as shown in Figure 2b–d, the presence of TEA led to the formation of smaller NH_2-MIL-125 crystals compared with those synthesized without TEA. Specifically, the thickness of NH_2-MIL-125(0.14) and NH_2-MIL-125(0.28) were 107.9 and 75.6 nm, respectively. As the concentration of TEA increased to 0.56 mol/L, the thickness was further reduced to 28.5 nm (Figure 2d). These observations underscore the importance of kinetic control of crystallization in modulating the size and thickness of the NH_2-MIL-125 crystals. Specifically, the introduction of TEA significantly promoted the deprotonation of NH_2-BDC ligands, thereby accelerating the rates of NH_2-MIL-125 nucleation. Moreover, anisotropic growth of NH_2-MIL-125 crystals was hindered by the increased steric hindrance of TEA, resulting in the formation of smaller MOF crystals with reduced lateral size and thickness. It was worth mentioning that adding TEA up to a concentration of 0.56 mol/L was optimal for promoting the formation of desired NH_2-MIL-125

https://doi.org/10.1021/cbe.4c00103
Chem Bio Eng. 2024, 1, 855–862

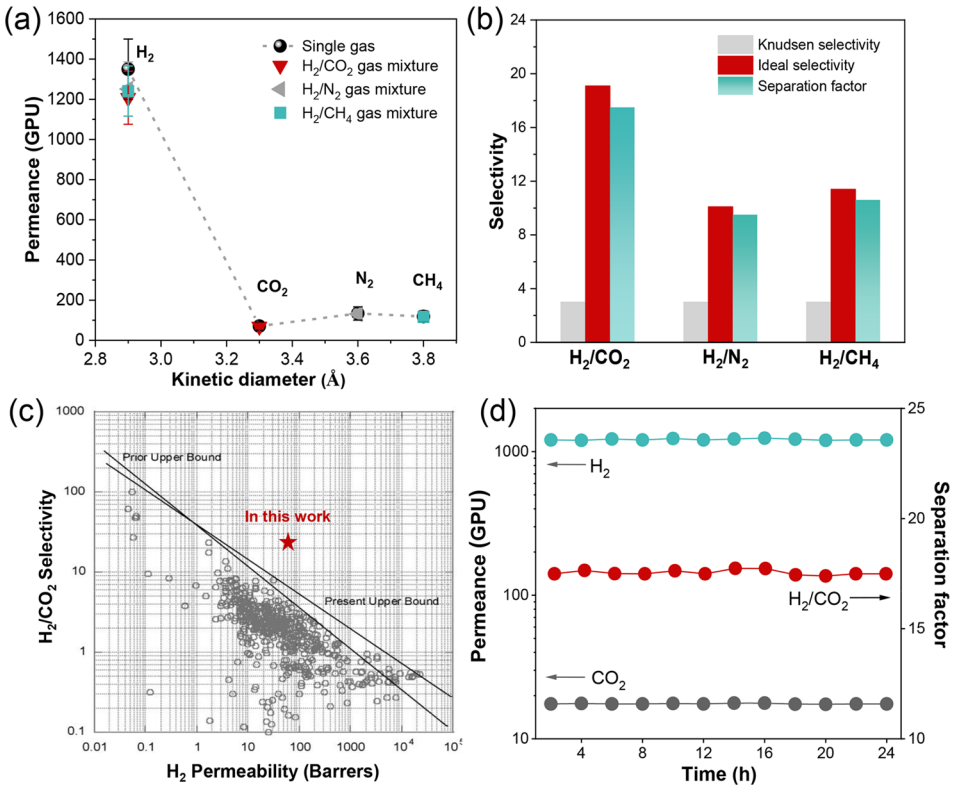

Figure 5. (a) Single and mixed gas permeances of NH_2-MIL-125 membrane measured under ambient conditions. (b) Ideal selectivity and separation factor of different gas pairs through the NH_2-MIL-125 membrane. (c) Comparison of the H_2/CO_2 separation performance of NH_2-MIL-125 membrane with 2008 upper bound line. (d) Long-term operation stability of H_2/CO_2 gas mixture on obtained NH_2-MIL-125 membrane at 1 bar and 25 °C.

nanosheets. Beyond this concentration, there was no longer a significant reduction in particle size (Figure S1). Relevant PXRD (Figure 2f) and FTIR (Figure 2g) measurements further revealed that diffraction patterns obtained under varying conditions matched well with the simulated pattern, ensuring the purity of the NH_2-MIL-125 phase.

3.2. Preparation of Ultrathin NH_2-MIL-125 Membrane. Subsequently, NH_2-MIL-125(0.56) NSs were deposited on porous α-Al_2O_3 substrate (Figure 3a) using a dynamic air−liquid interface-assisted self-assembly technique. Relevant SEM image demonstrated the formation of a uniform and closely packed seed layer (Figure 3b). The XRD pattern convincingly demonstrated a preferred *c*-orientation, as evidenced by the presence of only (002) and (004) diffraction peaks (Figure 4c). It should be noted that the above assembly process was sensitive to the water flow velocity, especially when smaller-sized NH_2-MIL-125(0.56) crystals.

The next step involved the epitaxial growth of *c*-oriented seed layers. There has been considerable advancement in oriented epitaxial growth of oriented MOF membranes over the past decade. Nevertheless, exerting precise control over growth kinetics of oriented seed layers, which is crucial for preparing ultrathin-oriented MOF membranes, remains in its infancy. Compared with conventional solvothermal method, utilizing single-mode microwave heating during epitaxial growth enabled not only dramatically reduced reaction duration but also much milder reaction conditions without sacrificing membrane continuity, thanks to its distinctive nonthermal effects. Relying on single-mode microwave heating, recently we achieved the fabrication of a *c*-oriented 500 nm thick NH_2-MIL-125 MOF membrane with outstanding H_2/CO_2 selectivity. In this study, we further extended the application of single-mode microwave heating to the epitaxial growth of NH_2-MIL-125(0.56) NS seed layers.

In addition, the metal source is found to significantly affect the kinetics of epitaxial growth. Initially, TPOT was utilized as a metal precursor. Nonetheless, its high reactivity triggered uncontrolled bulk nucleation, leading to pronounced crystal twinning in NH_2-MIL-125 membrane (Figure S2). Previous studies revealed that adopting two-dimensional transition metal sulfides, such as TiS_2, as metal source enabled significantly retarded bulk nucleation and therefore suppressed twinning in the membrane. In this research, TiS_2 was selected as the source of titanium. SEM images (Figure 3c) illustrated that the obtained membrane was well-intergrown. Nevertheless, achieving a delicate balance between twinning suppression and continuity maintenance remains a challenging task even under optimized reaction condition. For instance, decreasing TiS_2 concentration enabled effective twin suppression at the expense of a partial loss of membrane continuity due to insufficient nutrient supply (Figure 3d−f). The above results highlighted the need for exerting more precise control over release rate of metal source and therefore epitaxial growth kinetics.

The contra-diffusion synthetic protocol, which is featured with physical segregation of two precursor solutions containing metal ions and organic ligands, enabled concentration gradient-driven metal−ligand self-assembly, offering significant potential for the fabrication of ultrathin MOF membranes. This technique has garnered attention for its "self-regulating" capability, offering significant advantage in terms of ultrathin MOF membrane preparation.[31−34] Wang et al. pioneered the

https://doi.org/10.1021/cbe.4c00103
Chem Bio Eng. 2024, 1, 855−862

preparation of continuous ZIF-8 membrane using contra-diffusion technique.[35] Recently, a confined counterdiffusion strategy was further developed to enable epitaxial growth of (111)-oriented 165 nm thick UiO-66 membranes.[36] To be specific, trace amounts of ZrS_2, acting as the exclusive metal source, were deposited on the reverse side of a seed layer-coated porous α-Al_2O_3 substrate, which enabled controllable release and diffusion of the zirconium source. In this study, a confined counterdiffusion approach was further used in epitaxial growth of NH_2-MIL-125(0.56) NS monolayers under single-mode microwave heating. As shown in Figure 4a,b, a well-intergrown membrane with a thickness of only 80 nm was obtained after epitaxial growth. Simultaneously, only a diffraction peak assigned to the (002) plane could be discerned in the XRD pattern (Figure 4c), verifying the dominance of the *c*-preferred orientation. To the best of our knowledge, this is the thinnest oriented 3D MOF membrane reported in the literature.

Notable twin suppression could be attributed to the existence of concentration gradients that impede the uncontrolled diffusion of nutrients in the seed layer. In contrast to traditional epitaxial growth, effective segregation of NH_2-BDC ligand-containing solution and TiS_2 source by porous substrate creates concentration gradients of nutrients at the substrate−solution interface, ensuring steady supply of nutrients (i.e., Ti species and NH_2-BDC ligands) in intergranular spaces. Simultaneously, employing single-mode microwave heating not only promoted desired in-plane epitaxial growth but also inhibited undesired nucleation in bulk solution, owing to the unique nonthermal effect.

Simultaneously, utilizing exfoliated TiS_2 during epitaxial growth was proven to be crucial for facilitating lateral epitaxial growth with no compromise in membrane continuity. For comparison, bulk TiS_2 crystals were further attached to the back side of the seed layer-coated substrate while keeping other conditions unchanged. Our results indicated that substantial intercrystalline defects were generated, although crystal twinning could be effectively suppressed (Figure S3). Such a morphological discrepancy could be ascribed to different reactivities between bulk TiS_2 and exfoliated TiS_2 NSs. We inferred that TiS_2 exfoliation facilitated nucleophilic attack by NH_2-BDC ligands, favoring a more uniform and faster release of titanium species. In addition, we found that predeposition of oriented seed layer was indispensable for the formation of highly *c*-oriented ultrathin NH_2-MIL-125 membrane; otherwise, only the discontinuous NH_2-MIL-125 layer could be obtained (Figure S4).

3.3. Separation Performance for *c*-Oriented Ultrathin NH_2-MIL-125 Membrane. Finally, the separation performance of the obtained NH_2-MIL-125 membrane was evaluated through measuring volumetric flow rates of both single gases and binary gas mixtures with the Wicke−Kallenbach method (Figure S5). As shown in Figure 5a, H_2 displayed the highest permeance of the 1350 GPU, remarkably surpassing other larger-sized gases. Furthermore, our membrane exhibited exceptional ideal selectivity toward H_2/CO_2 (19.1), H_2/N_2 (10.1), and H_2/CH_4 (11.4) gas pairs, significantly exceeding the Knudsen selectivity (Figure 5b and Table S1). In particular, its H_2/CO_2 separation performance not only well surpassed state-of-the-art NH_2-MIL-125 membranes but also exceeded Robeson 2008 upper-bound limits for polymer membranes (Figure 5c and Table S2). Simultaneously, the H_2 permeance of our membrane surpassed that of all pure NH_2-MIL-125 membranes reported in the literature, highlighting the significance of concurrent manipulation of preferred orientation and membrane thickness in performance enhancement. Additionally, our online stability assessment revealed that our NH_2-MIL-125 membranes maintained consistent H_2/CO_2 separation performance over 24 h (Figure 5d), attesting to their robustness and reliability in practical applications.

The effect of the operating temperature on the separation performance was further investigated. It was observed that H_2 permeability continuously increased, while H_2/CO_2 selectivity slightly decreased with increasing operating temperature from 25 to 120 °C (Figure S6). This behavior can be attributed to gradually weakened affinity between the CO_2 and $-NH_2$ groups in the MOF framework at higher temperature.

4. CONCLUSIONS

To summarize, we successfully prepared a uniform NH_2-MIL-125 nanosheet based on the crystallization kinetics modulation approach with TEA as growth modulator. Moreover, through combining with single-mode microwave heating-assisted confined counter-diffusion-assisted epitaxial growth, oriented NH_2-MIL-125 membranes with a thickness of 80 nm were prepared. Concurrent use of confined counterdiffusion, exfoliated TiS_2 as titanium source, and single-mode microwave heating during epitaxial growth was found indispensable for retarding the growth rate in the vertical direction with no compromise in membrane continuity. Owing to the ultrathin thickness and high *c*-orientation, the prepared NH_2-MIL-125 membrane exhibited superior H_2/CO_2 separation performance with exceptional H_2 permeance, surpassing the state-of-the-art NH_2-MIL-125 membranes measured under similar conditions. Moreover, the synthetic protocol was proved to be reliable in terms of reproducibility.

■ ASSOCIATED CONTENT

Supporting Information

The Supporting Information is available free of charge at https://pubs.acs.org/doi/10.1021/cbe.4c00103.

Additional experimental details, materials, and methods, including characterization data and performance details (PDF)

■ AUTHOR INFORMATION

Corresponding Author

Yi Liu − *State Key Laboratory of Fine Chemicals, Frontiers Science Center for Smart Materials, School of Chemical Engineering, Dalian University of Technology, Dalian 116024, China;* orcid.org/0000-0002-2073-4832; Email: diligenliu@dlut.edu.cn

Authors

Yanwei Sun − *State Key Laboratory of Fine Chemicals, Frontiers Science Center for Smart Materials, School of Chemical Engineering, Dalian University of Technology, Dalian 116024, China; Faculty of Arts and Sciences, Beijing Normal University, Zhuhai 519087, China*

Jiahui Yan − *State Key Laboratory of Fine Chemicals, Frontiers Science Center for Smart Materials, School of Chemical Engineering, Dalian University of Technology, Dalian 116024, China*

Mingming Wu − *State Key Laboratory of Fine Chemicals, Frontiers Science Center for Smart Materials, School of*

https://doi.org/10.1021/cbe.4c00103
Chem Bio Eng. 2024, 1, 855−862

Chemical Engineering, Dalian University of Technology, Dalian 116024, China

Jie Jiang − *State Key Laboratory of Fine Chemicals, Frontiers Science Center for Smart Materials, School of Chemical Engineering, Dalian University of Technology, Dalian 116024, China*

Complete contact information is available at: https://pubs.acs.org/10.1021/cbe.4c00103

Notes

The authors declare no competing financial interest.

■ ACKNOWLEDGMENTS

We are grateful to National Natural Science Foundation of China (22108025, 22078039), Science Fund for Creative Research Groups of the National Natural Science Foundation of China (22021005), National Key R&D Program of China (2023YFB3810700), and the Fundamental Research Funds for the Central Universities (DUT22LAB602) for the financial support.

■ REFERENCES

(1) Kitagawa, S. Metal-organic frameworks (MOFs). *Chem. Soc. Rev.* **2014**, *43* (16), 5415−5418.

(2) Denny, M. S.; Moreton, J. C.; Benz, L.; Cohen, S. M. Metal−organic frameworks for membrane-based separations. *Nat. Rev. Mater.* **2016**, *1* (12), 16078.

(3) Qiu, S.; Xue, M.; Zhu, G. Metal-organic framework membranes: from synthesis to separation application. *Chem. Soc. Rev.* **2014**, *43* (16), 6116−6140.

(4) Qian, Q.; Asinger, P. A.; Lee, M. J.; Han, G.; Mizrahi Rodriguez, K.; Lin, S.; Benedetti, F. M.; Wu, A. X.; Chi, W. S.; Smith, Z. P. MOF-based membranes for gas separations. *Chem. Rev.* **2020**, *120* (16), 8161−8266.

(5) Hou, J.; Zhang, H.; Simon, G. P.; Wang, H. Polycrystalline advanced microporous framework membranes for efficient separation of small molecules and ions. *Adv. Mater.* **2020**, *32* (18), 1902009.

(6) Knebel, A.; Caro, J. Metal−organic frameworks and covalent organic frameworks as disruptive membrane materials for energy-efficient gas separation. *Nat. Nanotechnol.* **2022**, *17* (9), 911−923.

(7) Dan-Hardi, M.; Serre, C.; Frot, T.; Rozes, L.; Maurin, G.; Sanchez, C.; Férey, G. A new photoactive crystalline highly porous titanium(IV) dicarboxylate. *J. Am. Chem. Soc.* **2009**, *131* (31), 10857−10859.

(8) Friebe, S.; Mundstock, A.; Unruh, D.; Renz, F.; Caro, J. NH_2-MIL-125 as membrane for carbon dioxide sequestration: Thin supported MOF layers contra mixed-matrix-membranes. *J. Membr. Sci.* **2016**, *516*, 185−193.

(9) Sun, Y.; Song, C.; Guo, X.; Hong, S.; Choi, J.; Liu, Y. Microstructural optimization of NH_2-MIL-125 membranes with superior H_2/CO_2 separation performance by innovating metal sources and heating modes. *J. Membr. Sci.* **2020**, *616*, 118615.

(10) Sun, Y.; Liu, Y.; Caro, J.; Guo, X.; Song, C.; Liu, Y. -plane epitaxial growth of highly *c*-oriented NH_2-MIL-125(Ti) membranes with superior H_2/CO_2 selectivity. *Angew. Chem., Int. Ed.* **2018**, *130* (49), 16320−16325.

(11) Sun, Y.; Yan, D.; Wu, Y.; Shih, F.-Y.; Zhang, C.; Luo, H.; Lin, S.-H.; Liu, Y. Fabrication of twin-free ultrathin NH_2-MIL-125(Ti) membrane with *c*-preferred orientation using transition-metal trichalcogenides as titanium source. *ACS Mater. Lett.* **2022**, *4* (1), 55−60.

(12) Yoo, Y.; Lai, Z.; Jeong, H.-K. Fabrication of MOF-5 membranes using microwave-induced rapid seeding and solvothermal secondary growth. *Microp. Mesop. Mater.* **2009**, *123* (1-3), 100−106.

(13) Li, Y. S.; Bux, H.; Feldhoff, A.; Li, G. L.; Yang, W. S.; Caro, J. Controllable synthesis of metal-organic frameworks: From MOF nanorods to oriented MOF membranes. *Adv. Mater.* **2010**, *22* (30), 3322−3326.

(14) Ma, X.; Wan, Z.; Li, Y.; He, X.; Caro, J.; Huang, A. Anisotropic gas separation in oriented ZIF-95 membranes prepared by vapor-assisted in-plane epitaxial growth. *Angew. Chem., Int. Ed.* **2020**, *59* (47), 20858−20862.

(15) Pustovarenko, A.; Goesten, M. G.; Sachdeva, S.; Shan, M.; Amghouz, Z.; Belmabkhout, Y.; Dikhtiarenko, A.; Rodenas, T.; Keskin, D.; Voets, I. K.; Weckhuysen, B. M.; Eddaoudi, M.; de Smet, L. C. P. M.; Sudhölter, E. J. R.; Kapteijn, F.; Seoane, B.; Gascon, J. Nanosheets of nonlayered aluminum metal-organic frameworks through a surfactant-assisted method. *Adv. Mater.* **2018**, *30* (26), 1707234.

(16) Zhuang, L.; Ge, L.; Liu, H.; Jiang, Z.; Jia, Y.; Li, Z.; Yang, D.; Hocking, R. K.; Li, M.; Zhang, L.; Wang, X.; Yao, X.; Zhu, Z. A surfactant-free and scalable general strategy for synthesizing ultrathin two-dimensional metal-organic framework nanosheets for the oxygen evolution reaction. *Angew. Chem., Int. Ed.* **2019**, *58* (38), 13565−13572.

(17) Seoane, B.; Castellanos, S.; Dikhtiarenko, A.; Kapteijn, F.; Gascon, J. Multi-scale crystal engineering of metal organic frameworks. *Coord. Chem. Rev.* **2016**, *307*, 147−187.

(18) Stock, N.; Biswas, S. Synthesis of metal-organic frameworks (MOFs): routes to various MOF topologies, morphologies, and composites. *Chem. Rev.* **2012**, *112* (2), 933−969.

(19) Carpenter, B. P.; Talosig, A. R.; Rose, B.; Di Palma, G.; Patterson, J. P. Understanding and controlling the nucleation and growth of metal-organic frameworks. *Chem. Soc. Rev.* **2023**, *52*, 6918.

(20) Stavitski, E.; Goesten, M.; Juan-Alcañiz, J.; Martinez-Joaristi, A.; Serra-Crespo, P.; Petukhov, A. V.; Gascon, J.; Kapteijn, F. Kinetic control of metal-organic framework crystallization investigated by time-resolved in situ X-Ray scattering. *Angew. Chem., Int. Ed.* **2011**, *50* (41), 9624−9628.

(21) Shete, M.; Kumar, P.; Bachman, J. E.; Ma, X.; Smith, Z. P.; Xu, W.; Mkhoyan, K. A.; Long, J. R.; Tsapatsis, M. On the direct synthesis of Cu(BDC) MOF nanosheets and their performance in mixed matrix membranes. *J. Membr. Sci.* **2018**, *549*, 312−320.

(22) Guo, H.; Zhu, Y.; Wang, S.; Su, S.; Zhou, L.; Zhang, H. Combining coordination modulation with acid-base adjustment for the control over size of metal-organic frameworks. *Chem. Mater.* **2012**, *24* (3), 444−450.

(23) Hu, S.; Liu, M.; Guo, X.; Kuang, Z.; Li, K.; Song, C.; Zhang, G. Effect of titanium ester on synthesizing NH_2-MIL-125(Ti): Morphology changes from circular plate to octahedron and rhombic dodecahedron. *J. Solid State Chem.* **2018**, *262*, 237−243.

(24) Hu, S.; Liu, M.; Guo, X.; Li, K.; Han, Y.; Song, C.; Zhang, G. Effects of monocarboxylic acid additives on synthesizing metal-organic framework NH_2-MIL-125 with controllable size and morphology. *Cryst. Growth Des.* **2017**, *17* (12), 6586−6595.

(25) Hu, S.; Liu, M.; Li, K.; Song, C.; Zhang, G.; Guo, X. Surfactant-assisted synthesis of hierarchical NH_2-MIL-125 for the removal of organic dyes. *RSC Adv.* **2017**, *7* (1), 581−587.

(26) Hu, S.; Liu, M.; Li, K.; Zuo, Y.; Zhang, A.; Song, C.; Zhang, G.; Guo, X. Solvothermal synthesis of NH_2-MIL-125(Ti) from circular plate to octahedron. *CrystEngComm* **2014**, *16* (41), 9645−9650.

(27) Agrawal, K. V.; Topuz, B.; Pham, T. C. T.; Nguyen, T. H.; Sauer, N.; Rangnekar, N.; Zhang, H.; Narasimharao, K.; Basahel, S. N.; Francis, L. F.; Macosko, C. W.; Al-Thabaiti, S.; Tsapatsis, M.; Yoon, K. B. Oriented MFI membranes by gel-less secondary growth of sub-100 nm MFI-nanosheet seed layers. *Adv. Mater.* **2015**, *27* (21), 3243−3249.

(28) Jeon, M. Y.; Kim, D.; Kumar, P.; Lee, P. S.; Rangnekar, N.; Bai, P.; Shete, M.; Elyassi, B.; Lee, H. S.; Narasimharao, K.; Basahel, S. N.; Al-Thabaiti, S.; Xu, W.; Cho, H. J.; Fetisov, E. O.; Thyagarajan, R.; DeJaco, R. F.; Fan, W.; Mkhoyan, K. A.; Siepmann, J. I.; Tsapatsis, M. Ultra-selective high-flux membranes from directly synthesized zeolite nanosheets. *Nature* **2017**, *543* (7647), 690−694.

(29) Lu, X.; Yang, Y.; Zhang, J.; Yan, Y.; Wang, Z. Solvent-free secondary growth of highly b-oriented MFI zeolite films from

anhydrous synthetic powder. *J. Am. Chem. Soc.* **2019**, *141* (7), 2916−2919.
(30) Liu, Y.; Chen, S.; Ji, T.; Yan, J.; Ding, K.; Meng, S.; Lu, J.; Liu, Y. Room-temperature synthesis of zeolite membranes toward optimized microstructure and enhanced butane isomer separation performance. *J. Am. Chem. Soc.* **2023**, *145* (14), 7718−7723.
(31) Huang, K.; Li, Q.; Liu, G.; Shen, J.; Guan, K.; Jin, W. A ZIF-71 hollow fiber membrane fabricated by contra-diffusion. *ACS Appl. Mater. Interfaces* **2015**, *7* (30), 16157−16160.
(32) Wang, N.; Li, X.; Wang, L.; Zhang, L.; Zhang, G.; Ji, S. Nanoconfined zeolitic imidazolate framework membranes with composite layers of nearly zero thickness. *ACS Appl. Mater. Interfaces* **2016**, *8* (34), 21979−21983.
(33) Kwon, H. T.; Jeong, H.-K. In situ synthesis of thin zeolitic−imidazolate framework ZIF-8 membranes exhibiting exceptionally high propylene/propane separation. *J. Am. Chem. Soc.* **2013**, *135* (29), 10763−10768.
(34) Sun, Y.; Huang, H.; Guo, X.; Qiao, Z.; Zhong, C. Controlling metal ion counter diffusion in confined spaces for in situ growth of mixed metal MOF membranes for gas separation. *ChemNanoMat* **2019**, *5* (9), 1244−1250.
(35) Yao, J.; Dong, D.; Li, D.; He, L.; Xu, G.; Wang, H. Contra-diffusion synthesis of ZIF-8 films on a polymer substrate. *Chem. Commun.* **2011**, *47* (9), 2559−2561.
(36) Sun, Y.; Yan, J.; Gao, Y.; Ji, T.; Chen, S.; Wang, C.; Lu, P.; Li, Y.; Liu, Y. Fabrication of highly oriented ultrathin Zr-MOF membrane from nanosheets towards unprecedented gas separation. *Angew. Chem., Int. Ed.* **2023**, *62*, No. e202216697.

https://doi.org/10.1021/cbe.4c00103
Chem Bio Eng. 2024, 1, 855−862